

---

# Round Attention: A Novel Round-Level Attention Mechanism to Accelerate LLM Inference

---

Yaohua Tang\* Zhicheng Hu\* Kun Cheng\*  
Fan Mo Qiheng Lv Hua Wang<sup>†</sup> Zhi Chen<sup>‡</sup>

Moore Threads AI

## Abstract

The increasing context window size in large language models (LLMs) has improved their ability to handle complex, long-text tasks. However, as the conversation rounds continue, it is required to store a large amount of KV cache in GPU memory, which significantly affects the efficiency and even availability of the model serving systems. This paper analyzes dialogue data from real users and discovers that the LLM inference manifests a watershed layer, after which the distribution of round-level attention shows notable similarity. We propose Round Attention, a novel round-level attention mechanism that only recalls and computes the KV cache of the most relevant rounds. The experiments show that our method saves 55% memory usage without compromising model performance.

## 1 Introduction

Recent advancements in large language models have facilitated the wider adoption of language model services for everyday problem-solving tasks. However, prolonged interactions expose two significant challenges. First, the rapid expansion of context length incurs substantial computational overhead due to the quadratic scaling of self-attention mechanisms. Second, although key-value (KV) caching alleviates redundant computations, it substantially increases GPU memory requirements, resulting in limited inference batch sizes and GPU under-utilization. For instance, an NVIDIA A100 with 40GB of memory can accommodate only a single LLaMA request with a context length of 128K, spending nearly 50% of its processing time on KV cache access He and Zhai [2024].

To enhance inference efficiency, previous research has investigated KV cache eviction and sparse attention techniques for LLMs, noting that attention is inherently sparse. These methods either store the entire KV cache in GPU memory, selecting key tokens during autoregression to reduce cross-attention computation time Tang et al. [2024], or maintain the KV cache in CPU memory, transferring it to GPU memory token by token during inference Chen et al. [2024], Sun et al. [2024], He and Zhai [2024], Lee et al. [2024]. The former does not reduce GPU memory usage, while the latter incurs significant communication overhead. Furthermore, current methods often require an expensive calculation of the most relevant tokens for each layer.

The aforementioned studies analyze contextual relationships at the token level. Analysis in Sun et al. [2024] reveals that most post-RoPE keys exhibit high cosine similarity with adjacent tokens, enabling chunk-level approximations for selecting important tokens. LONGMEMEVAL benchmark Wu et al. [2024] explores the memory design options for memory-augmented chat assistants and discovers that round is “the best” granularity for storing and utilizing the interactive history. This aligns with

---

\*Equal contribution. tangyaohua28@gmail.com

<sup>†</sup>Corresponding author. wangtianyu.di@gmail.com

<sup>‡</sup>zhic@mthreads.com

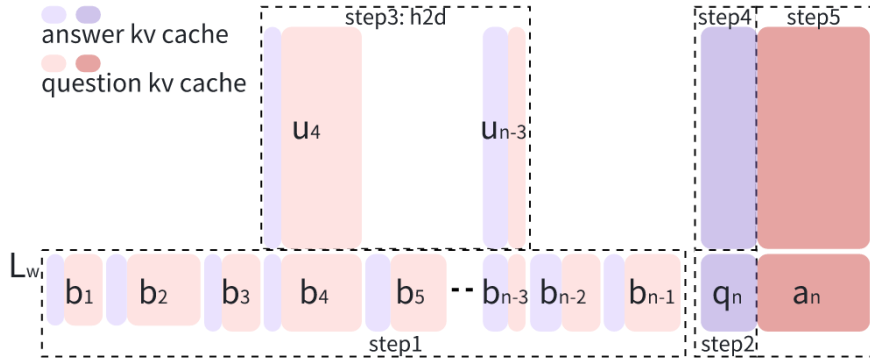


Figure 1: The inference pipeline of Round Attention. Our KV cache is managed and stored in a round-based manner. For a given token, the KV cache is divided into two tensors: the upper and lower halves. The complete KV cache is offloaded to CPU memory, while only the lower half tensor is retained in GPU memory. The upper half tensor is transferred from CPU memory to GPU memory at real-time based on query relevance, thereby optimizing memory usage.

the communication habits of individuals in real-life interactions, where rounds clearly express closer contextual relationships than tokens.

Therefore, we analyze the attention matrix using rounds and identify two interesting patterns. First, the attention score distributions at the round granularity in currently prevalent open-source large models exhibit considerable variability in the initial layers; however, from a certain layer onward, the distributions between layers become remarkably similar. Second, within a single dialogue round, the attention scores computed for the “question” in relation to previous dialogue turns closely resemble those computed for the “answer” corresponding to the same prior turns. With these discoveries, we propose **Round Attention**, a method that leverages the sparsity nature of the attention matrix. During inference, it incorporates only the most relevant rounds’ key-value (KV) cache into the attention computation while offloading the complete KV cache to CPU memory. Round Attention stores and transfers the KV cache at the round granularity, segmenting each round’s KV cache into two complete tensors. Due to the first identified pattern, we only need to compute the top-k rounds once at a specific layer and then perform a single host-to-device (h2d) operation to transfer the corresponding KV cache tensor to GPU memory. This approach contrasts with other methods that require top-k computations at each layer and transfer the KV cache at the token granularity, significantly reducing the latency overhead associated with top-k calculations and offloading mentioned in other approaches.

Our primary contributions are as follows:

- We dissect the attention patterns in LLM post-deployment at the round granularity and reveal two enlightening characteristics in attention matrix in real applications.
- Based on these characteristics, we design a novel method, Round Attention, associated with an array of techniques for long-context dialogues. This approach stores and transfers the KV cache at round granularity.
- We conduct extensive experiments on the proposed approach. The results show that it can reduce the GPU memory footprint by 55% with no accuracy loss. More importantly, thanks to the one-time top-k selection and host-to-device (h2d) transfer, our method achieves lower latency compared to standard non-offloaded Flash Attention.

## 2 Related Work

### 2.1 Attention Matrix Analysis

The sparsity of attention weights in pre-trained LLMs, especially in long-context scenarios, has been well-documented Liu et al. [2022], Ribar et al. [2023], Liu et al. [2023b], Xiao et al. [2023]. Ma

et al. [2024] investigate the distribution of important tokens in the context and discovered that recent tokens are more important than distant ones. They also find that attention scores between consecutive layers are similar, which has also been previously observed in smaller models Xiao et al. [2019], Bhojanapalli et al. [2021].

Mu et al. [2024] report that Attention weights were remarkably similar between the transformer layers, particularly the adjacent layers. Men et al. [2024] identify notable redundancy across LLM layers, where some layers contribute marginally to the model. Fan et al. [2024] show that for some tasks, LLMs can achieve results comparable to the final output at some intermediate layers.

## 2.2 KV Cache Eviction Algorithm

Many previous efforts focus on KV cache compression to accelerate attention and reduce memory usage. H2O Zhang et al. [2023] retains a limited budget for the important KV cache regarding the sum of historical attention scores. FastGen Ge et al. [2023] further categorizes tokens and only keeps partial KV cache using a more sophisticated strategy. TOVA Oren et al. [2024] simplifies the policy by determining the permanently discarded tokens using the current query. StreamingLLM Xiao et al. [2023] handles infinitely long text with attention sinks and a finite KV cache. SparQ Ribar et al. [2023] computes approximate attention scores by channel pruning and selects important tokens through them. Tang et al. [2024] concludes that the importance of a token is highly dependent on the query and proposes Quest, a method that records the *min* and *max* key values in KV cache pages and estimates the importance of a page using query vectors.

However, these approaches face several challenges. First, it is costly to identify the topk attention. For example, applying a naive search algorithm, e.g. IVF Douze et al. [2024], requires access over 30% key states to obtain the topk results Liu et al. [2024], which is quite compute-intensive. Second, these approaches save the KV cache in the GPU memory to avoid loading them from the CPU memory, which does not reduce the total memory consumption of KV cache, hence limiting the max context window and inference batch size.

Some papers attempted to offload KV cache to CPU memory to reduce the active GPU memory usage. Liu et al. [2024] proposes to build approximate nearest neighbor search (ANNS) indexes for KV vectors in CPU memory and retrieve the most relevant ones through vector search during generation. Sun et al. [2024] stores the low-rank key cache and offloads the value cache to reduce the memory footprint for larger batch sizes and longer sequences. Chen et al. [2024] stores the LSH hash tables and runs the attention computation on the CPU, which significantly reduces the workload of attention computation. However, these works transmit the key-value (KV) cache at the token level, and in some approaches, the top-k selection is computed on a per-layer basis, which implies that the KV cache is also transferred layer by layer, resulting in significant overhead for h2d transfers.

## 3 Methodology

This section presents Round Attention, a novel approach that dissects the attention matrix at the round level for multi-round dialogue tasks by taking  $\langle q, a \rangle$  pairs as the basic analysis unit. The objective is to reduce the memory footprint and inference latency without sacrificing the accuracy of LLMs. This section will also discuss a suite of techniques behind Round Attention.

### 3.1 Attention Distribution

Given an input sequence  $X = [x_1, x_2, \dots, x_n]$ , a standard Transformer Vaswani et al. [2023] network computes a set of queries  $Q$ , keys  $K$ , and values  $V$  using linear transformations on  $X$ . It then computes the self-attention scores as follows:

$$\text{Attention}(Q, K) = \text{softmax}\left(\frac{QK^T}{\sqrt{d_k}}\right) \quad (1)$$

To investigate the attention pattern among rounds, we denote the sum of the attention scores of the tokens in  $\mathbf{q}_n, \mathbf{a}_n$  and the tokens in  $\langle \mathbf{q}_k, \mathbf{a}_k \rangle$  of the previous  $k$ -th round for layer  $l$  as:

$$\text{qAttention}_k^l = \sum_{\substack{i \in \mathbf{q}_n \\ j \in \langle \mathbf{q}_k, \mathbf{a}_k \rangle}} \text{Attention}(Q_i^l, K_j^l) \quad (2)$$

$$\text{aAttention}_k^l = \sum_{\substack{i \in \mathbf{a}_n \\ j \in \langle \mathbf{q}_k, \mathbf{a}_k \rangle}} \text{Attention}(Q_i^l, K_j^l) \quad (3)$$

Denote the distribution of  $\text{qAttention}_k^l$  and  $\text{aAttention}_k^l$  as:

$$P_q^l = \frac{\text{qAttention}_k^l}{\sum_{i=1,2,\dots,n-1} \text{qAttention}_i^l} \quad (4)$$

$$P_a^l = \frac{\text{aAttention}_k^l}{\sum_{i=1,2,\dots,n-1} \text{aAttention}_i^l} \quad (5)$$

We examine the distribution patterns of  $P_q^l$  and  $P_a^l$  within the same layer, as well as the distribution patterns of  $P_q^l$  across different layers. SharedGPTShareGPT52K [2024], a dataset produced by conversations between real users and ChatGPT, is adopted to analyze the distribution patterns. Qwen2.5-0.5B Yang et al. [2024] is selected for demonstration.

**Observation 1: Attention distributions of  $q_n$  and  $a_n$  are similar.**

As an example, in Figure 2(a), we selected one dialogue comprising 85 rounds to analyze the attention probability distribution of the 85th round in relation to the preceding rounds across different layers. As shown in the figure, the trends of  $P_q^l$  and  $P_a^l$  are highly similar in each layer, indicating that rounds highly correlated with the question of the 85th round are also highly correlated with its answer. Thus, after performing prefill on the question of the 85th round, we can identify the most relevant historical rounds’ KV caches for AR computation based on the round attention distribution, rather than utilizing the KV caches from all rounds. We would like to emphasize that this pattern is not only applicable to this particular example. We have derived such pattern after analyzing a substantial number of dialogues, and we are using this example as a subject for analysis.

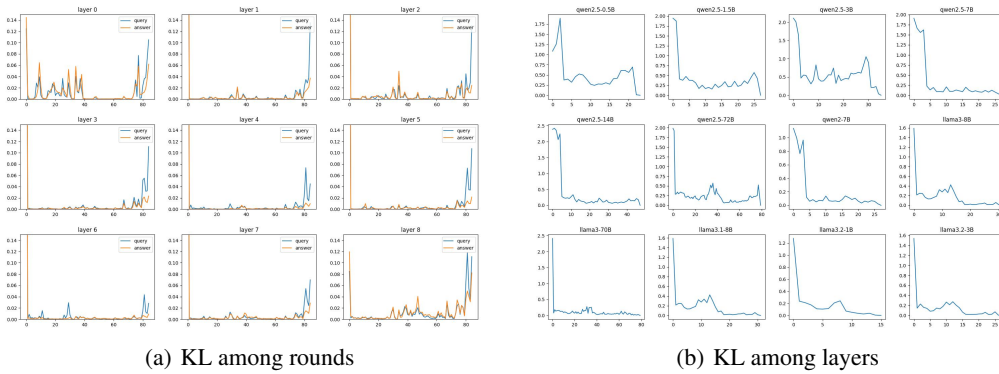


Figure 2: Round attention distribution patterns. **(a)** The horizontal axis represents the round index and the vertical axis represents the attention scores of  $q_n/a_n$  in relation to historical rounds. It can be observed that the variation trend of the attention scores calculated for  $q_n$  is highly similar to that of  $a_n$ . **(b)** The horizontal axis is the layer index. The vertical axis represents the average KL divergence between  $P_q^l$  of each layer and  $P_q^l$  of subsequent layers. It can be observed that nearly all mainstream models exhibit a similar pattern.

**Observation 2: Attention distributions among layers are similar.**

Next, we analyze the correlation of  $P_q^l$  across different layers. For a given layer, we compute the Kullback-Leibler (KL) divergence between that layer and each subsequent layer, averaging these

---

**Algorithm 1** Round Attention

---

**Input:**  $b_1 \dots b_{n-1}, u_1 \dots u_{n-1}$   
Initialize: transfer  $b_1 \dots b_{n-1}$  from host to device memory  
**for**  $i = n$  **to**  $\infty$  **do**  
  New query  $\mathbf{q}_n$ , conduct prefill calculation for layer  $1 \sim L_w$   
  Calculate TopK rounds based on  $\text{qAttention}^{L_w}$   
  transfer  $u_{topk}$  to device memory  
  finish prefill and AR calculation  
  transfer  $u_n$  to host memory  
**end for**  
transfer  $b_n \dots b_\infty$  to host memory

---

values to obtain the mean KL divergence between the layer and all following layers. We then plot these values for all layers, resulting in Figure 2(b). It can be observed that for nearly all currently mainstream open-source models, regardless of their size, a similar pattern emerges. The initial few layers exhibit significant differences compared to the subsequent layers; however, after reaching a certain layer, the disparity suddenly diminishes substantially. We designate this layer as “**watershed layer**”  $L_w$  and we list this layer for several open-source models in Appendix B. From this layer onward, the  $P_q^l$  values of the subsequent layers are very close to each other. Although there are occasional instances of slight increases in divergence, these differences remain significantly smaller than those observed in the earlier layers. This indicates that we can select the rounds most relevant to the question at the watershed layer for subsequent attention calculations, thereby eliminating the need to perform this selection computation at every layer, which would incur additional time costs. Based on these two observations, we propose our inference pipeline, Round Attention. We will provide a detailed description of this pipeline in the following sections.

### 3.2 Round Attention Inference Pipeline

Figure 1 depicts the pipeline for Round Attention. First, we design a strategy to determine the watershed layer for a given LLM. In real multi-turn dialogue LLM serving systems, it is impractical to store all historical KV caches from all users in the GPU memory. A user’s historical KV cache will normally be swapped out to the host memory or even slower storage devices when she is inactive for some period, so that the precious GPU memory can be well-utilized. For simplicity, we assume that the LLM has  $L$  layers.  $b_m$  denotes the KV cache of  $1 \sim L_w$  layers for the  $m$  dialogue round,  $u_m$  denotes the KV cache of  $L_w \sim L$  layers for the  $m$  dialogue round.  $b_m$  and  $u_m$  are stored as separate tensor in memory.

When the user becomes active, e.g. asking LLM the  $n$ -th question  $\mathbf{q}_n$ , the following steps will be executed to conduct the inference for this turn.

- step1: Load  $b_1 \dots b_{n-1}$  to the GPU memory from the host memory.
- step2: Performs prefill computation for  $\mathbf{q}_n$  using layer  $1 \sim L_w$ .
- step3: Select the most relevant TopK dialogue rounds via the strategies proposed in Section 3.3 with  $\text{qAttention}^{L_w}$ , and load the KV cache for layer  $L_{w+1} \sim L, u_{topk}$ .
- step4: Finish prefill for the remaining layers.
- step5: Decode  $\mathbf{a}_n$ .

Compared to the previous works that work on the token level, therefore invoking multiple fragmented KV cache transfers between host and device memory, our method works at the dialogue round level where a monolithic tensor for all tokens in prior rounds is transferred to GPU at once. Upon the accomplishment of the computation of  $u_n$  for layer  $L_{w+1} \sim L$  in the  $n$ -th round, the new KV cache is saved to the host memory as a monolithic tensor as well. Therefore, our methods reduces the number of expensive host-to-device(H2D) and device-to-host(D2H) data transferring. In addition, moving data in a large chunk is able to better utilize PCIe bandwidth. The algorithm is summarized in Algorithm 1.

### 3.3 Round Strategy

Three strategies are considered to determine the top  $k$  most relevant dialogue rounds after  $L_w$  is discovered and  $\text{qAttention}_k$  is computed.

**Strategy 1: Fixed rounds** selects the satisfied rounds using a predefined threshold, e.g.  $\text{qAttention}_k^{L_w} > v$ . Analyzing the distribution of attention scores across rounds we find that the attention values are concentrated in a limited number of rounds, with the majority of rounds exhibiting minimal attention scores. Based on this data distribution, we selected  $v = 0.1$ .

**Strategy 2: TopK rounds** picks that rounds that correspond to the top 10%  $\text{qAttention}_k^{L_w}$ . Analyzing the distribution of round attention scores reveals that the top 10% of rounds account for over 80% of the cumulative attention.

**Strategy 3: Adaptive rounds** chooses the rounds adaptively with the  $\text{qAttention}$  distribution. The condition is defined as:  $\text{qAttention}_k^{L_w} > \text{mean} + k * \text{std}$ , where  $\text{mean}$  and  $\text{std}$  are the mean and standard deviation of  $\text{qAttention}_k$ .

### 3.4 KV cache Dropping

We observed that the KV caches of some dialogue rounds in the ShareGPT are never active and do not affect the inference quality even if removed for attention computation. For these rounds, we delete the KV cache in the corresponding tokens to avoid saving them in memory. Further, it is unnecessary to load such KV cache from the host memory when they become active, hence saving storage and memory copy costs.

### 3.5 Memory and Performance Analysis

This section investigates the memory and performance of Round Attention.

**Memory footprint analysis.** Given an LLM with context length  $S$ , hidden size  $H$ , total layers  $L$ , and inference batch size  $B$ , the amount of memory consumed by the KV cache is calculated by Equation 6.

$$M_{orig} = 2 * 2 * B * S * H * L \quad (6)$$

where the first 2 represents K and V, and the second 2 means that float16 occupies 2 bytes.

For Round Attention, assuming that the  $K$  most relevant rounds are chosen from the total  $T$  rounds of dialogue, the amount of memory used by each round on average is shown in Equation 7.

$$M_{round} = 4B * S * H * L_w + 4B * K/T * S * H * (L - L_w) \quad (7)$$

This is because layer  $1 \sim L_w$  uses the entire KV cache, and the subsequent layers ( $L_{w+1} \sim L$ ) only compute the attention with the most relevant  $K$  rounds.

The memory saving ratio of Round Attention can be expressed as Equation 8.

$$\frac{M_{round}}{M_{orig}} = \frac{L_w + K * (L - L_w)/T}{L} = \frac{L_w}{L} + \frac{K}{T} * (1 - \frac{L_w}{L}) \quad (8)$$

Since  $K$  is much smaller than  $T$  in practice, e.g.  $6 \sim 8$  vs tens to hundreds, the upper bound of Equation 8 approximates to  $\frac{L_w}{L}$ . When  $K$  equals  $T$ , that is, all dialogue rounds are selected, Round Attention degrades to the original inference with virtually no memory cost. As shown in Table B, for currently mainstream large models, the ratio  $\frac{L_w}{L}$  ranges from 0.18 to 0.46, indicating a memory saving percentage of 54% to 82%, which is quite substantial.

**Latency analysis.** Latency of LLM inference is composed by prefill and decode. Prefill is compute bound and the total FLOPs can be approximate to  $2 * N * D$ , where  $N$  is the number of model parameters and  $D$  is the number of computed tokens. It can be measured by TTFT(time to first token), which is usually computed by Eq. (9) Korthikanti et al. [2022]. As autoregressive decoding is memory bound, the generation time of  $S$  tokens is close to the time it takes to load the entire KV cache (shown in Equation 6) from the GPU memory. Assuming that the GPU memory bandwidth is  $B_h$ , TPOT (time per output token) of the original inference pipeline is computed as Equation 10.

$$T_{tft} = 24B * S * L * H^2 * (1 + S/6H) \approx 24B * S * L * H^2 \quad (9)$$

$$T_{tpot} = 4B * S * H * L / B_h \quad (10)$$

Therefore, the latency of the original LLM with  $S$  output tokens is computed as  $L_{orig} = T_{tft} + T_{tpot}$ .

Recall that Round Attention first loads the tokens of the top  $k$  most relevant rounds of layers  $1 \sim L_w$  from the host memory (bandwidth  $B_l$ ), and then performs attention using these tokens. The latency is contributed by four major components: prefill of the first  $L_w$  layers, prefill of remaining layers using TopK relevant rounds, transferring of the TopK relevant KV cache to device memory, and AR of the remaining layers. Since data transferring can be asynchronous and hidden by prefill computation, we only consider the other three components as Equation 11.

$$L_{round} = \frac{24BSL_wH^2 + 24BL_wKS/TH^2}{C} + \frac{4BHS/TH(L - L_w)}{B_h} \quad (11)$$

where  $C$  and  $B_h$  are FP16 TFLOPs and memory bandwidth of a GPU, respectively.

The latency saving is  $\frac{L_{round}}{L_{orig}}$ , denoted as  $\frac{L_r}{L_o}$  in Equation 12 for simplicity.

$$\begin{aligned} \frac{L_r}{L_o} &= \frac{(1 + \frac{K}{T}) * \frac{6H}{C} * \frac{L_w}{L} + \frac{K}{T * B_h} * \frac{L - L_w}{L}}{\frac{1}{B_h} + \frac{6H}{C}} \\ &\approx \frac{1 + \frac{K}{T}}{\frac{L_w}{L}} + \frac{KC}{6THB_h} * \frac{L - L_w}{L} \\ &= (1 + (1 - \frac{C}{6HB_h}) * \frac{K}{T}) * \frac{L_w}{L} + \frac{KC}{6THB_h} \end{aligned} \quad (12)$$

The following conclusions can be safely drawn.

- The longer the context length ( $\frac{K}{T}$  is small), the more latency can be saved. For example, when  $\frac{K}{T}$  is negligible, the latency of Round Attention approximately equals to  $L_w/L$  of the original inference pipeline.
- The earlier the watershed layer  $L_w$  is present ( $\frac{L_w}{L}$  is small), the shorter the latency would be achieved.

## 4 Experiments And Analysis

### 4.1 Experiment Setting

This section evaluates the model accuracy, memory footprint, and inference performance of Round Attention.

**Data.** Two widely used datasets, ShareGPTShareGPT52K [2024] and LONGMEMEVALWu et al. [2024], are used to evaluate the effectiveness of Round Attention. ShareGPT contains a collection of approximately 52K user-shared conversations scraped through the ShareGPT API. These conversations are multi-turn, including both user prompts and responses from ChatGPT. LONGMEMEVAL is a comprehensive benchmark designed to evaluate five core long-term memory capabilities of commercial chat assistants: information extraction, multi-session reasoning, temporal reasoning, knowledge updates, and abstention. This benchmark also records the historical user-assistant conversations with 250 rounds on average. This is a difficult dataset, on which GPT-4o’s accuracy is only 0.5773.

**Baselines.** A suite of the latest open-source LLMs, e.g. Qwen2.5, LLaMA3, and LLaMA3.2 Grattafiori et al. [2024], are tested on the above datasets, but our approach can be applied to any other long-context LLMs. We use PyTorch and FlashAttentionDao et al. [2022] as the default inference framework, which are referred as Flash. All testing are conducted on a single Nvidia A100 GPU with 80GB of memory, equipped with PCIe. The CPU used was an Intel(R) Xeon(R) Gold 6346 CPU operating at 3.10GHz (1.16/3.60GHz), and the system had 1TB of memory.

### 4.2 Accuracy Evaluation

We classify ShareGPT into four categories with respect to dialogue rounds, `mini` (0-10 rounds), `small` (10-30 rounds), `medium` (30-50 rounds), and `large` (50-100 rounds). We treat the last

prompt in each category as  $\mathbf{q}_n$ , and then use the default inference framework and Round Attention to compute  $\mathbf{a}_n$ . GPT-4o is employed as the Judge to evaluate the quality of the generated results. Each  $\mathbf{a}_n$  is evaluated 5 times and the average score is taken as the final score of the response. The prompts are chosen from AlignBenchLiu et al. [2023a], where the samples can be found in Appendix A.

Table 1: Accuracy for Qwen2.5-3B under different round strategies

		Flash	TopK	Fixed	Adaptive
Mini	score	7.51	7.5	7.33	7.5
	tokens	809	515	560	515
Small	score	7.49	7.47	7.48	7.5
	tokens	4339	1245	1245	1245
Medium	score	7.42	7.5	7.5	7.48
	tokens	11491	1276	1089	1089
Large	score	7.49	7.46	7.43	7.4
	tokens	19548	2343	1142	1639
Ave	score	7.477	<b>7.483</b>	7.435	7.470

As shown in Table 1, the TopK strategy is the most effective, with an average score exceeding that of the standard inference engine. This indicates that using only the KV caches from the TopK rounds doesn't have notable impact on the quality of model responses, as the attention matrix is highly sparse, particularly for the extremely large conversational rounds. Furthermore, the number of tokens we processed was reduced by 88% compared to the standard inference engine for large rounds, which suggests a substantial decrease in attention computation and a significant saving in GPU memory.

Table 2: Accuracy for different Model under the TopK round strategy

Attribute	Small		Medium		Large	
	score	tokens	score	tokens	score	tokens
Flash	6.39	4339	5.95	11491	5.8	19548
Qwen2.5-0.5B	5.74	1245	5.85	1199	6.06	2391
Flash	7.77	4339	7.8	11491	7.44	19548
Qwen2.5-7B	7.08	1218	7.49	1382	7.57	2448
Flash	7.45	4260	4.05	11735	3.01	19812
Llama3-8B	7.6	1227	3.84	1695	3.47	3376
Flash	7.35	4260	7.11	11735	7.38	19812
Llama3.1-8B	7.39	1212	7.17	1369	7.46	2477

To validate the generalize ability of this method, we test the accuracy on various sizes of the Qwen2.5 model, as well as on some models from Llama3 and Llama3.2. All experiments employed the TopK round strategy. The results are presented in Table 2. It is evident that the overall scores of the responses generated by our method on these models are comparable to those produced by the standard inference engine. However, we also observe that for the Qwen-2.5 series models, the accuracy of Round Attention may decrease with fewer rounds. In contrast, when the number of rounds exceeds 50, Round Attention consistently outperforms Flash Attention.

Since the responses from ShareGPT are subjective, we also utilize the objective dataset, LONGMEMEVAL, as the test bench to further validate the effectiveness of our approach. The original LONGMEMEVAL benchmark evaluate the results yielded by Llama3-8B. For consistency purpose, we also run tests on the same model. To showcase the generalization of our approach, we conduct the same experiments on Qwen2.5-7B as well.

As shown in Table 3, despite the challenging nature of LONGMEMEVAL, Round Attention performs remarkably well. For the Llama 3-8B model, Round Attention is comparable to Flash Attention, whereas for the Qwen 2.5-7B model, the accuracy of Round Attention is twice that of Flash Attention.

Table 3: Accuracy for Llama3-8B on LONGMEMEVAL Benchmark

	Llama3-8B		Qwen2.5-7B	
	Flash	Round	Flash	Round
Single-session-user	0.2714	0.2857	0.1	0.2286
Knowledge-update	0.4872	0.4744	0.2821	0.4872
multi-session	0.1353	0.0977	0.0376	0.1353
temporal-reasoning	0.1504	0.1729	0.0752	0.1429
Single-session-assistant	0.5357	0.4821	0.2321	0.4464
Single-session-preference	0.0	0.0333	0.0	0.1333
Accuracy	0.25	0.242	0.114	0.24

Interestingly, in the temporal reasoning tasks, Round Attention consistently outperforms Flash Attention, indicating that excessive information can lead to interference in reasoning tasks. Identifying the key rounds allows for more accurate inference results.

### 4.3 GPU Memory Reduction and Latency Reduction

To empirically evaluate the latency of Round Attention compared to Flash Attention, we selected 20 dialogue samples from each of the four categories mentioned earlier. Each sample was run 10 times, and the average latency was computed and plotted in Figure 3.

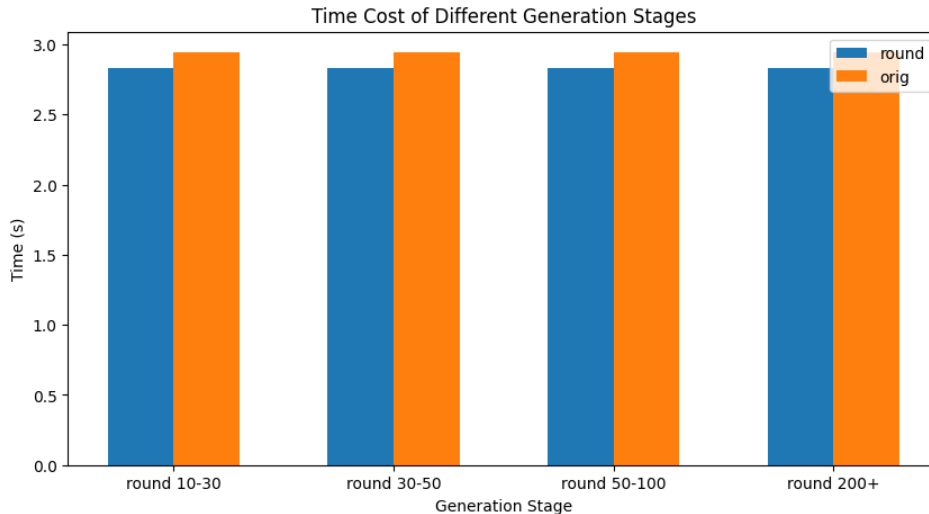


Figure 3: The statistical results of end-to-end inference time for Round Attention compared to Flash Attention across different round categories.

It can be observed that for all different round categories, the latency of Round Attention is lower than that of Flash Attention. This improvement is due to our KV cache storage and transfer strategy, which keeps the h2d transfer time manageable, and our top-k selection is computed only once rather than at each layer. We provide a detailed breakdown of latency in the Appendix C. Due to the h2d transfer and the selection of top-k, the latency during the  $q_n$  prefill phase exhibits a slight peak at layer  $L_w$ ; however, this peak is minor and occurs only once. In contrast, during the  $a_n$  decode phase, the reduction in the KV cache leads to decreased attention computation time. As the number of decode steps increases, this reduction accumulates and ultimately surpasses the one-time overhead from the h2d transfer and top-k selection, resulting in an overall latency that is superior to that of Flash Attention.

#### 4.4 Round vs Token

In this section, we compare the two granularities. For both granularities, we employed the same top-k calculation strategy to retrieve the KV cache. Specifically, we first computed the average attention score for all tokens/rounds at each granularity, selecting those with attention scores greater than the average. The model used for testing was Llama3.1-8B. The results are presented in Table 4. It is evident that, with the same top-k calculation strategy, the recall accuracy at the round granularity surpasses that of the token granularity. This is particularly pronounced in the Single-session-assistant task, where the answers reside within several sessions. The recall at the round granularity effectively retrieves the most relevant sessions, whereas the recall at the token granularity is dispersed across multiple sessions, resulting in a significantly lower accuracy compared to the round granularity.

Table 4: Accuracy for two granularities.

	token	round
Single-session-user	0.2857	0.2857
Knowledge-update	0.2	0.3333
multi-session	0.1111	0.1111
temporal-reasoning	0.1481	0.1111
Single-session-assistant	0.1818	0.4545
Single-session-preference	0.0	0.0
Accuracy	0.16	0.2

## 5 CONCLUSION AND DISCUSSION

In the context of real-world applications providing services with large language models (LLMs), the historical key-value (KV) cache accumulates as users engage in increasingly lengthy dialogue exchanges. We propose that, during inference with such extended dialogue rounds, employing a round-based approach offers a more effective means of managing the KV cache and handling interactions with historical information. Through an analysis of the attention matrix patterns at the round granularity, we observed that contemporary large models exhibit a watershed layer, beyond which the distribution of round-based attention becomes remarkably similar. This observation allows us to compute the most relevant rounds for subsequent layers’ attention calculations just once at the watershed layer. Consequently, we can significantly reduce GPU memory usage while effectively limiting the time required for selection. By storing the KV cache based on rounds, we can transfer all necessary KV cache data to GPU memory in a single host-to-device (h2d) operation, thereby minimizing the time overhead associated with h2d transfers. We validated the effectiveness of our approach through experiments, demonstrating that it is able to significantly reduce inference latency, with inference accuracy remaining largely consistent with that of the full KV cache.

### Limitations

This section discusses some limitations this paper has that we intentionally leave as the future work to further improve.

Limitation 1: Offloading to memory incurs additional memory overhead. Although memory is significantly cheaper and larger than GPU memory, it still adds extra overhead to the system.

Limitation 2: While Round Attention reduces GPU memory usage, out-of-memory (OOM) issues may still arise when the number of dialogue rounds reaches a certain threshold. This indicates that Round Attention alone cannot fundamentally resolve the GPU memory issues associated with very long dialogues. It needs to be combined with other techniques to effectively address memory problems, such as the continuous dropping of infrequently used key-value caches mentioned in Section 3.4. Additionally, various other key-value cache compression and dropping strategies can be utilized in combination to tackle GPU memory issues in practical dialogue systems.

Limitation 3: The benefits of serving are limited for scenarios with shorter dialogue rounds, making it more suitable for longer user dialogue interactions.

## References

- Srinadh Bhojanapalli, Ayan Chakrabarti, Andreas Veit, Michal Lukasik, Himanshu Jain, Frederick Liu, Yin-Wen Chang, and Sanjiv Kumar. Leveraging redundancy in attention with reuse transformers. [arXiv preprint arXiv:2110.06821](https://arxiv.org/abs/2110.06821), 2021.
- Zhuoming Chen, Ranajoy Sadhukhan, Zihao Ye, Yang Zhou, Jianyu Zhang, Niklas Nolte, Yuandong Tian, Matthijs Douze, Leon Bottou, Zhihao Jia, et al. Magicpig: Lsh sampling for efficient llm generation. [arXiv preprint arXiv:2410.16179](https://arxiv.org/abs/2410.16179), 2024.
- Tri Dao, Daniel Y. Fu, Stefano Ermon, Atri Rudra, and Christopher Ré. Flashattention: Fast and memory-efficient exact attention with io-awareness, 2022. URL <https://arxiv.org/abs/2205.14135>.
- Matthijs Douze, Alexandr Guzhva, Chengqi Deng, Jeff Johnson, Gergely Szilvassy, Pierre-Emmanuel Mazaré, Maria Lomeli, Lucas Hosseini, and Hervé Jégou. The faiss library, 2024. URL <https://arxiv.org/abs/2401.08281>.
- Siqi Fan, Xin Jiang, Xiang Li, Xuying Meng, Peng Han, Shuo Shang, Aixin Sun, Yequan Wang, and Zhongyuan Wang. Not all layers of llms are necessary during inference. [arXiv preprint arXiv:2403.02181](https://arxiv.org/abs/2403.02181), 2024.
- Suyu Ge, Yunan Zhang, Liyuan Liu, Minjia Zhang, Jiawei Han, and Jianfeng Gao. Model tells you what to discard: Adaptive kv cache compression for llms. [arXiv preprint arXiv:2310.01801](https://arxiv.org/abs/2310.01801), 2023.
- Aaron Grattafiori, Abhimanyu Dubey, Abhinav Jauhri, Abhinav Pandey, Abhishek Kadian, Ahmad Al-Dahle, Aiesha Letman, and et al. The llama 3 herd of models, 2024. URL <https://arxiv.org/abs/2407.21783>.
- Jiaao He and Jidong Zhai. Fastdecode: High-throughput gpu-efficient llm serving using heterogeneous pipelines. [arXiv preprint arXiv:2403.11421](https://arxiv.org/abs/2403.11421), 2024.
- Vijay Korthikanti, Jared Casper, Sangkug Lym, Lawrence McAfee, Michael Andersch, Mohammad Shoeybi, and Bryan Catanzaro. Reducing activation recomputation in large transformer models, 2022. URL <https://arxiv.org/abs/2205.05198>.
- Wonbeom Lee, Jungi Lee, Junghwan Seo, and Jaewoong Sim. Infinigen: Efficient generative inference of large language models with dynamic kv cache management, 2024. URL <https://arxiv.org/abs/2406.19707>.
- Di Liu, Meng Chen, Baotong Lu, Huiqiang Jiang, Zhenhua Han, Qianxi Zhang, Qi Chen, Chengruidong Zhang, Bailu Ding, Kai Zhang, et al. Retrievalattention: Accelerating long-context llm inference via vector retrieval. [arXiv preprint arXiv:2409.10516](https://arxiv.org/abs/2409.10516), 2024.
- Liu Liu, Zheng Qu, Zhaodong Chen, Fengbin Tu, Yufei Ding, and Yuan Xie. Dynamic sparse attention for scalable transformer acceleration. *IEEE Transactions on Computers*, 71(12):3165–3178, 2022.
- Xiao Liu, Xuanyu Lei, Shengyuan Wang, Yue Huang, Zhuoer Feng, Bosi Wen, Jiale Cheng, Pei Ke, Yifan Xu, Weng Lam Tam, Xiaohan Zhang, Lichao Sun, Hongning Wang, Jing Zhang, Minlie Huang, Yuxiao Dong, and Jie Tang. Alignbench: Benchmarking chinese alignment of large language models, 2023a.
- Zichang Liu, Jue Wang, Tri Dao, Tianyi Zhou, Binhang Yuan, Zhao Song, Anshumali Shrivastava, Ce Zhang, Yuandong Tian, Christopher Re, et al. Deja vu: Contextual sparsity for efficient llms at inference time. In *International Conference on Machine Learning*, pages 22137–22176. PMLR, 2023b.
- Da Ma, Lu Chen, Situo Zhang, Yuxun Miao, Su Zhu, Zhi Chen, Hongshen Xu, Hanqi Li, Shuai Fan, Lei Pan, et al. Compressing kv cache for long-context llm inference with inter-layer attention similarity. [arXiv preprint arXiv:2412.02252](https://arxiv.org/abs/2412.02252), 2024.

- Xin Men, Mingyu Xu, Qingyu Zhang, Bingning Wang, Hongyu Lin, Yaojie Lu, Xianpei Han, and Weipeng Chen. Shortgpt: Layers in large language models are more redundant than you expect. [arXiv preprint arXiv:2403.03853](#), 2024.
- Yongyu Mu, Yuzhang Wu, Yuchun Fan, Chenglong Wang, Hengyu Li, Qiaozhi He, Murun Yang, Tong Xiao, and Jingbo Zhu. Cross-layer attention sharing for large language models. [arXiv preprint arXiv:2408.01890](#), 2024.
- Matanel Oren, Michael Hassid, Nir Yarden, Yossi Adi, and Roy Schwartz. Transformers are multi-state rnns. [arXiv preprint arXiv:2401.06104](#), 2024.
- Luka Ribar, Ivan Chelombiev, Luke Hudliss-Galley, Charlie Blake, Carlo Luschi, and Douglas Orr. Sparq attention: Bandwidth-efficient llm inference. [arXiv preprint arXiv:2312.04985](#), 2023.
- ShareGPT52K, 2024. URL <https://huggingface.co/datasets/RyokoAI/ShareGPT52K>.
- Hanshi Sun, Li-Wen Chang, Wenlei Bao, Size Zheng, Ningxin Zheng, Xin Liu, Harry Dong, Yuejie Chi, and Beidi Chen. Shadowkv: Kv cache in shadows for high-throughput long-context llm inference. [arXiv preprint arXiv:2410.21465](#), 2024.
- Jiaming Tang, Yilong Zhao, Kan Zhu, Guangxuan Xiao, Baris Kasikci, and Song Han. Quest: Query-aware sparsity for efficient long-context llm inference. [arXiv preprint arXiv:2406.10774](#), 2024.
- Ashish Vaswani, Noam Shazeer, Niki Parmar, Jakob Uszkoreit, Llion Jones, Aidan N. Gomez, Lukasz Kaiser, and Illia Polosukhin. Attention is all you need, 2023. URL <https://arxiv.org/abs/1706.03762>.
- Di Wu, Hongwei Wang, Wenhao Yu, Yuwei Zhang, Kai-Wei Chang, and Dong Yu. Longmemeval: Benchmarking chat assistants on long-term interactive memory, 2024. URL <https://arxiv.org/abs/2410.10813>.
- Guangxuan Xiao, Yuandong Tian, Beidi Chen, Song Han, and Mike Lewis. Efficient streaming language models with attention sinks. [arXiv preprint arXiv:2309.17453](#), 2023.
- Tong Xiao, Yinqiao Li, Jingbo Zhu, Zhengtao Yu, and Tongran Liu. Sharing attention weights for fast transformer. [arXiv preprint arXiv:1906.11024](#), 2019.
- An Yang, Baosong Yang, Beichen Zhang, Binyuan Hui, Bo Zheng, Bowen Yu, Chengyuan Li, Dayiheng Liu, Fei Huang, Haoran Wei, Huan Lin, Jian Yang, Jianhong Tu, Jianwei Zhang, Jianxin Yang, Jiayi Yang, Jingren Zhou, Junyang Lin, Kai Dang, Keming Lu, Keqin Bao, Kexin Yang, Le Yu, Mei Li, Mingfeng Xue, Pei Zhang, Qin Zhu, Rui Men, Runji Lin, Tianhao Li, Tingyu Xia, Xingzhang Ren, Xuancheng Ren, Yang Fan, Yang Su, Yichang Zhang, Yu Wan, Yuqiong Liu, Zeyu Cui, Zhenru Zhang, and Zihan Qiu. Qwen2.5 technical report. [arXiv preprint arXiv:2412.15115](#), 2024.
- Zihao Ye, Lequn Chen, Ruihang Lai, Yilong Zhao, Size Zheng, Junru Shao, Bohan Hou, Hongyi Jin, Yifei Zuo, Liangsheng Yin, Tianqi Chen, and Luis Ceze. Accelerating self-attentions for llm serving with flashinfer, February 2024. URL <https://flashinfer.ai/2024/02/02/introduce-flashinfer.html>.
- Zhenyu Zhang, Ying Sheng, Tianyi Zhou, Tianlong Chen, Lianmin Zheng, Ruisi Cai, Zhao Song, Yuandong Tian, Christopher Ré, Clark Barrett, et al. H2o: Heavy-hitter oracle for efficient generative inference of large language models. [Advances in Neural Information Processing Systems](#), 36: 34661–34710, 2023.

## A GPT-4 judged prompt

```
You are an assistant skilled in evaluating text quality.
Please assess the quality of an AI assistant's response to a
user's question as an impartial judge. You need to evaluate
the response based on the following dimensions:
We will provide historical chat information, which consists
of the content from previous multi-turn conversations between
the user and the assistant. We will give you the current
user's question and the AI assistant's response. When
you begin your evaluation, you need to follow the process
outlined below:
1. Evaluate the AI assistant's response from different
dimensions, and after assessing each dimension, assign a
score from 1 to 10 for each dimension.
2. Finally, based on the evaluations from each dimension,
provide an overall score from 1 to 10 for the AI assistant's
response.
3. Your scoring needs to be as strict as possible, and you
must adhere to the following scoring rules: Generally, the
higher the quality of the model's response, the higher the
score. Among the dimensions, factual accuracy and meeting
user needs are the most important, and the scores for these
two dimensions will dominate the final overall score.
When the model's response contains irrelevant information,
has fundamental factual errors, or generates harmful content,
the total score must be between 1 and 2.
When the model's response has no serious errors and is
generally harmless, but is of low quality and does not meet
user needs, the total score should be between 3 and 4.
When the model's response generally meets user requirements
but performs poorly in some dimensions, resulting in an
average quality, the total score can be between 5 and 6.
When the model's response quality performs well across all
dimensions, the total score should be between 7 and 8.
Only when the model's response quality fully addresses the
user's questions and all needs, and performs nearly perfectly
across all dimensions, can it receive a score of 9 to 10.
As an example, a reference answer can receive a score of 8.
Return all your evaluations and scoring results in the
following dictionary format (including parentheses), and
ensure that your scores are integers:
{'dimension 1': score, 'dimension 2': score, ..., 'overall
score': score}}, for example: {'factual accuracy': 9,
'meeting user needs': 6, ..., 'overall score': 7}}.
Historical chat information: {review}
User's question: {instruction}
[Assistant's response start]
{response}
[Assistant's response end]
```

## B Layer-W

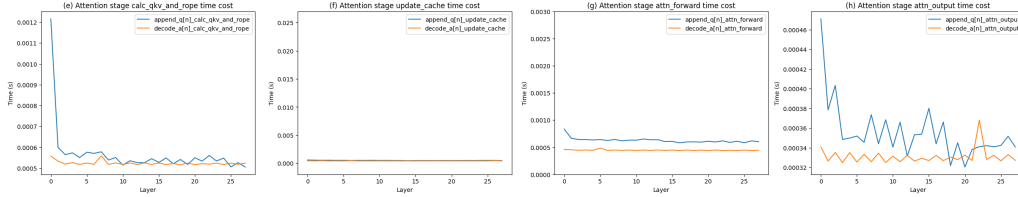
Here, we present the values of  $L_w$  obtained from several mainstream open-source models in Table 5.

Table 5:  $L_w$  for several models

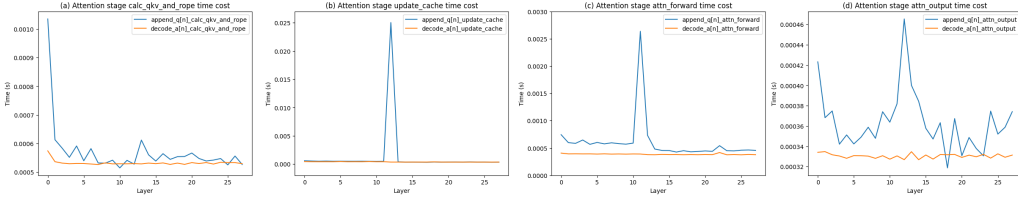
Model	size	$L$	$L_w$	save ratio
Qwen2.5	0.5B	24	11	54%
	1.5B	28	13	54%
	3B	36	12	67%
	7B	28	10	64%
	14B	42	19	55%
Llama3	72B	80	18	78%
	8B	28	5	82%
Llama3.2	70B	28	5	82%
	1B	16	5	69%
	3B	28	5	82%

## C Latency decomposition analysis

In the transformer architecture, the forward computation of attention is divided into four steps: `calc_qkv_and_rope`, `update_cache`, `attn_forward`, and `attn_output`. Our algorithm primarily modifies the `update_cache` and `attn_forward` steps. We analyze the execution times of step 2, step 3, step 4, and step 5 from Figure 1. Steps 2, 3, and 4 correspond to the prefill phase of  $q_n$ , which we refer to as the append phase, following the methodology outlined in Flash Infer Ye et al. [2024]. Step 5 represents the decode phase for  $a_n$ . We selected five examples from 50 to 100 rounds and conducted 100 experiments, plotting the trend of the average time for these two phases as a function of layer, resulting in Figure 4.



(a) Latency decompose for Flash Attention



(b) Latency decompose for Round Attention

Figure 4: Latency decomposition

From the figures, it can be observed that the execution times for round attention for the `calc_qkv_and_rope` and `attn_output` steps closely align with those of Flash Attention. The primary differences arise in the `update_cache` and `attn_forward` steps. Notably, the trends for these two steps remain consistent until layer  $L_w$ , where a divergence from Flash Attention emerges starting at layer 11.

In the append phase, as shown in Figure 4(b)(b), there is a noticeable peak in `update_cache` at layer 11, indicating two sources of overhead: one related to the computational cost of the top-k selection strategy, and the other pertaining to the h2d transfer time of the selected rounds' KV cache to the GPU memory. Similarly, Figure 4(b)(c) reveals a peak in the `attn_forward` step at layer 11, which also corresponds to the computational cost of the top-k strategy. It is evident that both the time taken for top-k computation and the h2d transfer time are relatively small.

Moving on to the decode phase, Round Attention demonstrates its advantages. The yellow lines in Figures 4(b)(b) and 4(b)(c) show a decline starting from layer 11, reflecting the reduced time for `update_cache` and `attn_forward` due to the shorter length of the KV cache.

Overall, the time overhead introduced by Round Attention occurs only once at layer  $L_w$ , while the benefits in the decode phase accumulate with an increasing number of decode steps. Ultimately, these advantages offset the additional time incurred, resulting in a lower overall execution time for Round Attention compared to Flash Attention.

## D GPU Memory decomposition analysis

In the experiments presented in Section C, we synchronously monitored the variations in GPU memory usage. The GPU memory consumption was measured using the `'torch.cuda.allocated_memory'` function.

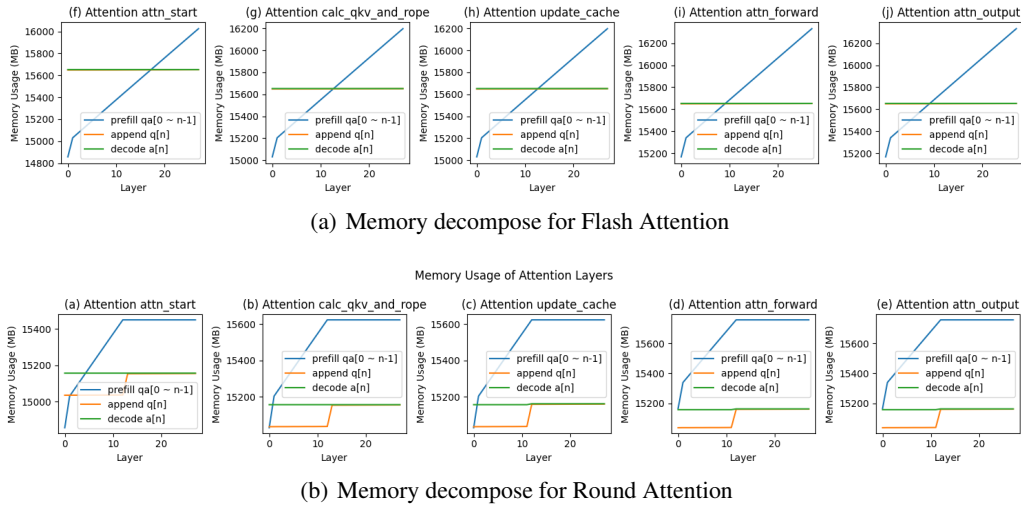


Figure 5: Latency decomposition

As illustrated in Figure 5, Flash Attention exhibits a slight increase in memory usage during the append and decode phases, although the magnitude is minimal. Conversely, for Round Attention, there is a noticeable increase in GPU memory usage after the 11th layer during the append phase, attributed to the selection and host-to-device transfer processes within the algorithm. Additionally, both the append and decode phases show a consistent overhead of several megabytes after the 11th layer, which is allocated for storing intermediate results of the selection process.

It is also evident that Round Attention exhibits lower GPU memory usage during both the append and decode phases compared to Flash Attention.